LA-UR-15-21476
Approved for public release; distribution is unlimited.

Title:	Magnifying Lenses with Weak Achromatic Bends for High-Energy Electron Radiography
Author(s):	Walstrom, Peter Lowell
Intended for:	For internal LANL use and for informing SLAC collaborators in electron radiography experiments at SLAC
Issued:	2015-02-27

Magnifying Lenses with Weak Achromatic Bends for High-Energy Electron Radiography

P. L. Walstrom

February 23, 2015

1 Abstract

This memo briefly describes bremsstrahlung background effects in GeV-range electron radiography systems and the use of weak bending magnets to deflect the image to the side of the forward bremsstrahlung spot to reduce background. The image deflection introduces first-order chromatic image blur due to dispersion. Two approaches to eliminating the dispersion effect to first order by use of magnifying lens with achromatic bends are described. Also, higher-order image blur terms caused by weak bends are also discussed, and shown to be negligibly small in most cases of interest.

2 Motivation

In GeV-range electron radiography (eRAD), bremsstrahlung from the test object, collimators, and any other solid objects struck by the beam contributes a significant unwanted background component to detected images, since most detectors being considered for electron radiography, although selected for sensitivity to high-energy electrons in the primary beam, are also sensitive to high-energy bremsstrahlung photons. This includes scintillators, which presently the detector type used in proton radiography and for electron radiography experiments planned for the Stanford Linear Accelerator (SLAC) ESTB facility in 2015. The bremsstrahlung photons from a thin object (i.e. an object with thickness much less than a radiation length), regardless of energy, are mostly contained in a cone of angular radius $1/\gamma$ around the primary electron direction at the point of bremsstrahlung production. For 10 GeV electrons, the characteristic bremsstrahlung cone angle is 5×10^{-5} radians. The actual radiation cone angle is larger than this because of multiple Coulomb scattering of the primary electrons in the object before they emit bremsstrahlung (angular spread due to beam emittance should be much smaller than the MCS spread in a properly designed electron radiography setup). Since in a typical electron radiography experiment the rms MCS angle will be on the order of a few times 10^{-4} radians, the

MCS angle will in most cases be larger than the intrinsic bremsstrahlung photon angular distribution width. Finally, the incident beam's chromatic matching angles can be still larger than the MCS angles; for example, with a matching correlation k_x of 1 m^{-1}, the matching angle for a point in the object a distance of 1 mm from the beam/lens axis is 1 milliradian. If there is no collimation of the bremsstralung photons downstream of the object, the bremsstralung beam spot width at 25 m from the test object (a typical object-detector distance in 10 GeV eRAD) for this matching angle will be roughly 5 cm for a 2 mm wide test object. However, the angle-cut collimator, designed to stop 10 GeV primary beam electrons, also is an effective collimator for bremsstrahlung photons, although it generates additional bremsstrahlung photons from electrons that graze the collimator's inside surfaces. The size of the aperture that is used in the angle-cut collimator depends on the beam energy of the experiment, the lens layout, and the object thickness in radiation lengths, but a typical aperture in 10 GeV eRAD is less than a millimeter in width. The z position (z is the beam axis) of the collimator the so-called Fourier point, which depends upon lens layout and matching conditions. In the initial version of the ESTB experiment, a slightly diverging chromatically unmatched beam, for which the Fourier point is downstream of the last of four lens quadrupoles, will be used. For this configuration, the bremsstrahlung beam spot at the object after collimation by the angle-cut collimator is typically a few millimeters wide. Recent Geant4 runs by Dan Poulson and Joseph Fabritius of P-25, which modeled electron images with bremsstrahlung background effects in the planned eRAD experiments in ESTB, gave results consistent with the above picture.

In any case, whether the beam illuminating the test object is matched or unmatched, one way to reduce bremsstrahlung background in the image is to deflect the image electrons to the side of the forward bremsstrahlung spot with a weak bending magnet, which ideally would be placed downstream of the collimator. If the bending magnet is placed before some of the lens quadrupoles, those quadrupoles should be centered on the angled beam axis coming out of the dipole to avoid beam steering by the quadrupoles.

Addition of a bending magnet to a magnetic lens introduces image blur-effects that do not occur in straight-axis lenses. The largest such effect is first-order dispersion. In addition to dispersion, a bend introduces second-order geometric aberrations that do not occur in straight-axis lenses. In straight-axis quadrupole lenses, the only geometric aberrations are of third order (providing the quadrupoles do not have sextupole field errors or skew field components due to roll-type misalignments). However, the second-order geometric aberrations in lenses with bends are small for small bend angles.

In this memo, two approaches to design of quadrupole magnetic lenses with bends that are achromatic, i.e. for which first-order dispersion blur in the image is zero, are described. Also, the second-order geometric aberrations caused by the bends and their scaling with bend angle are described.

3 Dispersion effects

In general, the vector of final six phase-space variables $\mathbf{z}^f$ in a lens system can be expressed as a Taylor series in the initial six phase space variables, denoted by the 6-vector $\mathbf{z}^i$. The transfer map code Marylie uses the canonical deviation variables $z_1 = x$, $z_2 = P_x = p_x/p_0$, $z_3 = y$, $z_4 = P_y = p_y/p_0$, $z_5 = \tau = c(t - t_0)$, and $z_6 = \delta = (E_0 - E)/p_0c$, where p_0 is the magnitude of the reference three-momentum and E_0 the reference kinetic energy. The map code COSY Infinity also uses canonical deviation variables, with the same z_1 through z_4, but different z_5 and z_6. In systems with bends, the transverse coordinates x and y refer to a system with axes rotated and translated such that the reference trajectory has $x = 0$, $P_x = 0$, $y = 0$, and $P_y = 0$. Normally, the reference particle has phase-space coordinates somewhere near the middle of the phase-space volume to be tracked.

Note that the commonly used angle variables x' and y' (in TRACE-3D, etc.) are non-canonical. That is, x, x' and y, y' are not canonically conjugate pairs, but x, p_x and y, p_y are. When p_x and p_y are divided by the constant p_0, the resultant z_2 and z_4 remain canonically conjugate to x and y, respectively. In the small-angle approximation, which is very good here, $x' = p_x/p$ and $y' = p_y/p$. Therefore $z_2 = (p/p_0)x'$ and $z_4 = (p/p_0)y'$. It is important to convert x' and y' to their canonical counterparts when evaluating the transfer map beyond the first order. In COSY, $z_6 = (E - E_0)/E_0$. Note the difference in sign between the Marylie and COSY z_6. At GeV electron energies the Marylie and COSY z_5 and z_6 are about the same, except for sign. Through third order, we can write for the transfer map that relates final to initial phase-space coordinates of a particle that has passed through a magnetic lens,

$$z_i^f = \sum_{j=1}^{6} R_{i,j} z_j^0 + \sum_{j=1}^{6}\sum_{k=1}^{6} T_{i,j,k} z_j^0 z_k^0 + \sum_{j=1}^{6}\sum_{k=1}^{6}\sum_{l=1}^{6} U_{i,j,k,l} z_j^0 z_k^0 z_l^0 \qquad (1)$$

We see from Eq. 1 that to lowest order, the final 6-D phase-space coordinates are linear and homogeneous in the initial coordinates (there are no constant terms in the map, since we use deviation coordinates). The second-order transfer-map terms are represented by the double summation and the third-order terms by the triple summation in Eq. 1. In this memo, the canonical coordinates of the charged-particle beam-transport code Marylie are used. The linear part of Eq. 1 can be written in matrix form, i.e.,

$$\begin{pmatrix} x^f \\ P_x^f \\ y^f \\ P_y^f \\ \tau^f \\ P_\tau^f \end{pmatrix} = \begin{pmatrix} R_{1,1} & R_{1,2} & R_{1,3} & R_{14} & R_{1,5} & R_{1,6} \\ R_{21} & R_{2,2} & R_{2,3} & R_{2,4} & R_{2,5} & R_{2,6} \\ R_{3,1} & R_{3,2} & R_{3,3} & R_{3,4} & R_{3,5} & R_{3,6} \\ R_{4,1} & R_{4,2} & R_{4,3} & R_{4,4} & R_{4,5} & R_{4,6} \\ R_{5,1} & R_{5,2} & R_{5,3} & R_{5,4} & R_{5,5} & R_{5,6} \\ R_{6,1} & R_{6,2} & R_{6,3} & R_{6,4} & R_{6,5} & R_{6,6} \end{pmatrix} \begin{pmatrix} x^0 \\ P_x^0 \\ y^0 \\ P_y^0 \\ \tau^0 \\ P_\tau^0 \end{pmatrix} \qquad (2)$$

The matrix of Eq. 2 is commonly called the R matrix. In a magnetostatic system with no skew field components in the quadrupoles (e.g., components

introduced by quadrupole roll, or rotation around the magnet axis), and with bends in the x plane only, many of the elements in Eq. 2 are zero, some are one, and the R matrix has the form

$$\begin{pmatrix} x^f \\ P_x^f \\ y^f \\ P_y^f \\ \tau^f \\ P_\tau^f \end{pmatrix} = \begin{pmatrix} R_{1,1} & R_{1,2} & 0 & 0 & 0 & R_{1,6} \\ R_{2,1} & R_{2,2} & 0 & 0 & 0 & R_{2,6} \\ 0 & 0 & R_{3,3} & R_{3,4} & 0 & 0 \\ 0 & 0 & R_{4,3} & R_{4,4} & 0 & 0 \\ R_{5,1} & R_{5,2} & 0 & 0 & 1 & R_{5,6} \\ 0 & 0 & 0 & 0 & 0 & 1 \end{pmatrix} \begin{pmatrix} x^0 \\ P_x^0 \\ y^0 \\ P_y^0 \\ \tau^0 \\ P_\tau^0 \end{pmatrix} \tag{3}$$

R_{16} and R_{26} are called the dispersion matrix elements, since final x and P_x depend on energy deviation if these elements are non-zero. If the R matrix is for the entire lens from the object plane to the image plane, we want $R_{1,6}$ to be zero to avoid first-order image blur due to energy spread; $R_{2,6}$ can be non-zero since it affects only the image-plane x angle, not the electron's final x. I call a magnetic transport system with $R_{1,6} = 0$ but $R_{2,6}$ non-zero a partial first-order achromat. The achromats discussed in this paper are all so-called partial achromats. For a straight-axis magnetostatic system with no skew field components in the quadrupoles, the R matrix is still simpler:

$$\begin{pmatrix} x^f \\ P_x^f \\ y^f \\ P_y^f \\ \tau^f \\ P_\tau^f \end{pmatrix} = \begin{pmatrix} R_{1,1} & R_{1,2} & 0 & 0 & 0 & 0 \\ R_{2,1} & R_{2,2} & 0 & 0 & 0 & 0 \\ 0 & 0 & R_{3,3} & R_{3,4} & 0 & 0 \\ 0 & 0 & R_{4,3} & R_{4,4} & 0 & 0 \\ 0 & 0 & 0 & 0 & 1 & R_{5,6} \\ 0 & 0 & 0 & 0 & 0 & 1 \end{pmatrix} \begin{pmatrix} x^0 \\ P_x^0 \\ y^0 \\ P_y^0 \\ \tau^0 \\ P_\tau^0 \end{pmatrix} \tag{4}$$

Note that not only are the dispersion elements $R_{1,6}$ and $R_{2,6}$ zero in the straight (no-bend) system, but the time-of-flight matrix elements $R_{5,1}$ and $R_{5,2}$ are also zero. $R_{5,6}$ remains non-zero in the straight system since the time of flight depends on the velocity, which varies with energy. As we shall see $R_{5,2}$ is usually zero in achromatic lenses with bends. Although $R_{5,1}$ is not zero in our achromats, the time spread $\tau = ct$ due to $R_{5,1}x$ in a lens system with a weak bend typically is on the order of microns and negligible from the point of view of motion blur in the image. Finally, even if $R_{1,6}$ is made to be zero in a lens with a bend, its energy derivative $T_{1,6,6}$ is not in general zero, but in most cases of interest to eRAD this particular second-order aberration is negligibly small.

4 Analytic approach to finding achromatic lenses with bends

In order to have a focused lens, we require $R_{1,2}$ and $R_{3,4}$ to both be zero in the transfer map from the object plane to the image plane. Typically, we also want to have equal or nearly equal magnification M in both x and y, i.e. $R_{1,1} = M_x$, $R_{3,3} = M_y$, where $|M_x| \approx |M_y|$ (it is OK for the signs of M_x and M_y to be

different, but we usually we want their magnitude to be the same). Finally, for high-quality images in lens systems with bends, we want $R_{1,6} = 0$ in order to eliminate first-order dispersion. This is a total of five conditions. One approach to solving this problem might be to simply use the fitting loop in a transfer-map code like Marylie to find a set of quadrupole-magnet gradients, lengths, and spacings that give an R matrix that satisfies the 5 conditions. In practice, this purely empirical approach usually fails, unless one can find a set of initial values for the quadrupole strengths and spacings that are close to the final values. We therefore hope to find guidance in solving the problem from the theory of differential equations.

We start by noting that in a system with bends in the x plane, in the linear approximation, we can describe the particle's x-plane deviation from the x-plane reference orbit as the linear combination of three basis rays: the so-called cosine-like, sine-like, and dispersion rays. For the y coordinate, the linear optics is the same as in a system with no bends and the y dispersion ray is identically zero. In straight systems, the basis rays are parameterized by the longitudinal coordinate z; in systems with bends, the parameter is arc length s along the reference trajectory. Also, in systems with bends, the transverse deviation coordinates x and y are in a reference frame that rotates such that the local $x - y$ plane is perpendicular to the reference trajectory. If we consider the R matrix elements to be functions of s, the cosine-like ray is $R_{1,1}(s)$, the sinelike ray $R_{1,2}(s)$, and the dispersion ray $R_{1,6}(s)$. In terms of these rays, an arbitrary ray in the x plane is $x(s) = R_{1,1}(s)x^0 + R_{1,2}(s)P_x^0 + R_{16}(s)\delta$, where x^0 and P_x^0 are the respective values of these quantities for $s = 0$. We note that there is no superscript on the energy deviation δ since particle energies do not change as they pass through magnetostatic systems. The R matrix at $s = 0$ is the identity matrix. Also, $dR_{1,1}(s)/ds = R_{2,1}(s)$, $dR_{1,2}(s)/ds = R_{2,2}(s)$, and $dR_{1,6}(s)/ds = R_{2,6}(s)$. Since at $s = 0$ the R matrix is the identity matrix, we have $R_{1,1}(0) = 1$, $dR_{1,1}/ds(0) = 0$, $R_{1,2}(0) = 0$, and $dR_{1,2}/ds(0) = 1$. Also, $R_{1,6}(0) = 0$ and $R_{2,6}(0) = 0$.

The theory of differential equations [1] tells us how to find the dispersion ray, if we know the sinelike and cosinelike rays. Eq. 5.25 in Ref. [1], which is the Green's function solution to the dispersion ray, reads

$$d_x(t) = s_x(t) \int_0^t c_x(\tau)h(\tau)d\tau - c_x(t) \int_0^t s_x(\tau)h(\tau)d\tau \tag{5}$$

The function $h(\tau)$ is the inverse of the radius of curvature, so $h(\tau) = qB_y(\tau)/p^0 = B_y(\tau)/B\rho$ (everywhere in this memo $B\rho$ refers to the so-called magnetic rigidity of the reference particle, *not* the rigidity of an arbitrary particle). We now note that Carey in Ref. [1] uses $\delta p/p_0$ for his energy deviation variable, but Marylie uses $-\delta E/p_0 c$. Therefore, in order to put Eq. 5 into Marylie units we need an overall factor of $-1/\beta$. Also, to avoid confusing arc length with time we use s instead of t and s' instead of τ. Then, using $R_{1,1}(s)$ for $c_x(t)$, etc. , we get,

instead of Eq. 5,

$$R_{1,6}(s) = \frac{-1}{\beta\ B\rho}\left[R_{1,2}(s)\int_0^s R_{1,1}(s')B_y(s')ds' - R_{1,1}(s)\int_0^s R_{1,2}(s')B_y(s')ds'\right] \tag{6}$$

If we need the s derivative of the dispersion (i.e. $R_{2,6}$), the appropriate expression is

$$R_{2,6}(s) = \frac{-1}{\beta\ B\rho}\left[R_{22}(s)\int_0^s R_{21}(s')B_y(s')ds' - R_{21}(s)\int_0^s R_{2,2}(s')B_y(s')ds'\right] \tag{7}$$

Finally, if the system is focused at arc length s, $R_{1,2}(s) = 0$, and

$$R_{16}(s) = \frac{1}{\beta\ B\rho}R_{11}(s)\int_0^s R_{12}(s')B_y(s')ds' \tag{8}$$

Inspection of Eq. 8 now tells us how to design magnifying lenses that are "partially" achromatic (i.e. $R_{1,6} = 0$ but $R_{2,6}$ is not necessarily zero), which is what we want for electron radiography systems with weak bends to deflect the image away from the bremsstrahlung spot. That is, we just have to somehow make the integral in Eq. 8 zero. The easiest way to do this is to center the bending magnet at an x focus location.

5 First approach: single-stage achromatic magnifier with an intermediate x focus between the third and fourth quadrupoles

This achromatic weak-bend magnifier has five quadrupoles (quadrupole doublet-drift-quadrupole triplet) followed by a long drift to the image plane. Therefore it will be called the "doublet-triplet achromat" in this memo. It has a magnification of $+10$ in x and -10 in y. We put an intermediate x focus between the second and third quadrupoles and place the center of the weak bending dipole at the intermediate x focus. This makes the integral of Eq. 8 zero.

This solution to the problem was found by breaking the problem into two steps. The first step was to set the doublet to give an intermediate x focus after the second quadrupole. The quadrupole doublet was chosen to have equal-length quadrupoles with equal but opposite-sign gradients. In order to get the intermediate x focus after the second quadrupole, the gradient of the first quadrupole has to be negative (i.e. the first quadrupole defocuses in x and the second quadrupole focuses in x). For this part of the problem there was one fitting aim, $R_{1,2} = 0$, so only one parameter had to adjusted by Marylie. The parameter adjusted was the drift length from the second quadrupole to the intermediate x focus.

There was one slight complication to the procedure. Unfortunately, Marylie does not allow the user to specify the dipole length; instead bend angle and field strength are specified. Therefore, when setting the drift length for the

intermediate x focus, it was necessary to split the bending dipole into two equal halves and place the first half after the drift following the second quadupole and use the Marylie fitting loop to set the $R_{12} = 0$ at the end of the half-length dipole. The second half-dipole was placed at the start of the second part of the overall lens. This guaranteed that entire dipole (both halves combined) was exactly centered on the intermediate x focus. The next step was to find triplet quadrupole settings and final drift length to the image plane that satisfied the four conditions $R_{1,2} = 0$, $R_{3,4} = 0$, $R_{1,1} = M_x$, and $R_{3,3} = M_y$, with $M_x = 10$, $M_y = -10$ (as it turned out, this combination of signs for the magnifications was the "natural" choice for this configuration). The four parameters adjusted in the Marylie fitting loop were the three gradients of the quadrupoles of the triplet and the final drift length. As expected, when the four conditions were satisfied, the achromatic condition $R_{16} = 0$ was also satisfied (to machine precision), as predicted by Eq. 8. This is shown by the object-plane-to-image-plane R matrix computed by Marylie after the fit loop converged:

```
 1.00000E+01 -3.99680E-15  0.00000E+00  0.00000E+00  0.00000E+00 -1.74166E-15
 5.26184E-01  1.00000E-01  0.00000E+00  0.00000E+00  0.00000E+00  2.60834E-04
 0.00000E+00  0.00000E+00 -1.00000E+01  2.48690E-14  0.00000E+00  0.00000E+00
 0.00000E+00  0.00000E+00 -2.66336E-01 -1.00000E-01  0.00000E+00  0.00000E+00
-2.60834E-03 -1.73764E-16  0.00000E+00  0.00000E+00  1.00000E+00  1.39694E-08
 0.00000E+00  0.00000E+00  0.00000E+00  0.00000E+00  0.00000E+00  1.00000E+00
```

It is interesting that, as a sort of by-product, the R matrix element R_{52} is also zero, although R_{51} is not. We recall that for straight-axis systems both R_{51} and R_{52} are automatically zero, but in general, for systems with bends, R_{51} and R_{52} are both non-zero. Fig. 1 shows four rays for the doublet-triplet achromatic lens: the x and y-plane chromatically matched rays [2], and the x and y-plane sinelike rays (which have been multiplied by a small initial angle to make them fit in the figure). Quadrupole pole pieces are indicated by the black rectangles. The dipole is not shown, but it is centered at the point where the purple curve crosses the axis. For future reference, the beamline parameters for this example are listed in the table below. The total bend angle is 0.2 degrees, or about 3.5 milliradians. This gives an image displacement of about 9 cm. The dipole field is unrealistically high; this was done to keep the dipole short for ray plotting purposes. The beam energy was 13.65 GeV. The design is by no means optimized, but is a proof of the concept.

Although the doublet-triplet achromat is a first-order (partial) achromat, it still has the second-order chromatic aberrations of straight-axis magnifiers. It is of interest to compare the size of the four second-order coefficients $T_{1,1,6}$, $T_{1,2,6}$, $T_{3,3,6}$, and $T_{1,2,6}$. For the straight-axis system, we take the 13.65 GeV "Russian" quadruplet $\times 10$ magnifier for the SLAC ESTB eRAD proof-of-principle experiment. The second order chromatic coefficients for the double-triplet achromat and the Russian quadruplet are given in Table II below. Since both lenses have a magnification of 10, it is not necessary to divide them by the magnification in the comparison. With matching, the second-order chromatic blur is dominated by $T_{1,2,6}$ and $T_{3,4,6}$. We see that $T_{1,2,6}$ is larger for the achromat than the Russian quadruplet by a factor of 2.5, and $T_{3,4,6}$ larger by a factor of 2.7. It may

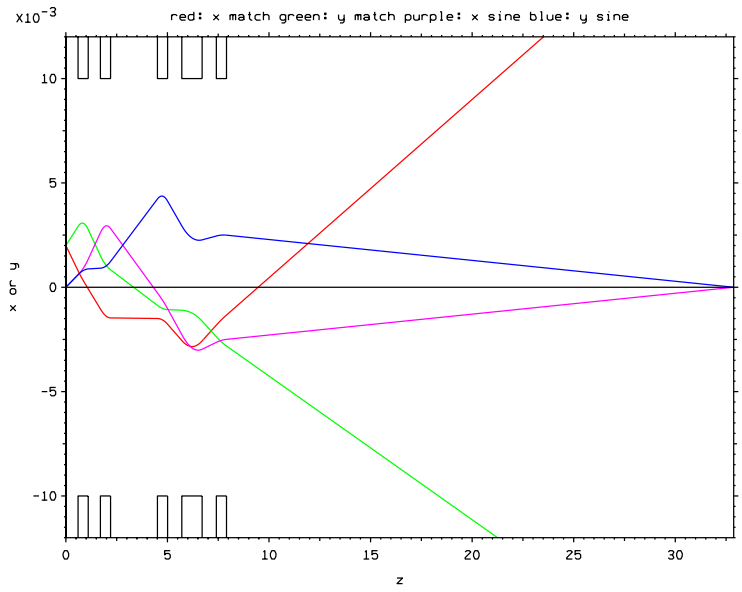

Figure 1: Ray plot for the doublet-triplet achromatic-bend magnifier. Red curve: x-plane matched ray; green curve: y-plane matched ray; purple curve: x-plane sinelike ray; blue curve: y-plane sinelike ray.

Table I: Beamline for an achromatic lens with an intermediate x focus

Element name	element type	length (m)	bending field (T)	gradient (T/m)
f1	drift	0.6	—	—
q1	quadrupole	0.5	—	-110
q1q2spac	drift	0.6	—	—
q2	quadrupole	0.5	—	110
q2bspace	drift	2.09778	—	—
bend	dipole	0.016	10.0	—
dab	drift	0.2	—	—
q3	quadrupole	0.5	—	-63.2583
d34	drift	0.7	—	—
q4	quadrupole	1.0	—	36.3882
d45	drift	0.7	—	—
q5	quadrupole	0.5	—	-13.33417
dfinal	drift	25.0883	—	—

Table II: Comparison of second-order chromatic aberration coefficients

coefficient	Russian quadruplet value	achromat value
$T_{1,1,6}$	-14.7	140.4
$T_{1,2,6}$	-55.1	139.0
$T_{3,3,6}$	-15.9	64.2
$T_{3,4,6}$	-31.2	-84.3

be possible to reduce these ratios somewhat by optimizing the achromat design, but the achromat will be worse in any case because of the greater length of the part of the lens from the start of q1 to the end of q5. For a particular achromat, the four chromatic aberration coefficients $T_{1,1,6}$, $T_{3,2,6}$, $T_{3,3,6}$ and $T_{3,4,6}$ are very nearly independent of bend angle (for weak bends with negligible edge focusing) and are essentially the same as those of the equivalent straight lenses where the bends are replaced by drifts of the same length.

As mentioned previously, adding the bend dipole to the lens introduces second-order geometric aberrations that are not present in straight lenses. The second-order geometric aberrations affecting final x are $T_{1,1,1}$, $T_{1,1,2}$, $T_{1,3,3}$, $T_{1,3,4}$, and $T_{1,4,4}$. The second-order geometric aberrations affecting final y are fewer: $T_{3,1,3}$, $T_{3,1,4}$, $T_{3,2,3}$, and $T_{3,2,4}$. The aberrations affecting x are plotted against bending angle in Fig. 2 and the aberrations affecting y in Fig. 3. It can be seen that they all have a linear dependence on bend angle. To get a rough idea of their effect on a typical image, we can take $T_{3,1,3}$ and $T_{3,2,4}$. $T_{3,1,3}$ is the largest coefficient multiplying two initial lengths and $T_{3,2,4}$ the largest multiplying an angle and a length. If we take x_0 =1 mm and also y_0 =1 mm, we get from the $T_{3,1,3}$ term $\delta y = 0.5$ micron for the largest bend angle of 0.2 degrees. But we must divide this by the magnification of 10, so the y displacement referred to the object due to this term is about 0.05 microns. However, since this term involves two initial lengths, it does not blur the image; it just distorts it slightly. Terms like $T_{3,2,3}$ involving an initial angle, however, do blur the image, since there is multiple Coulomb scattering (matching angles combined with $T_{3,2,3}$ do not blur the image- they just distort it, since the matching angles are a linear function of the initial transverse position in the object). For an MCS rms x angle of 1 milliradian and an initial y of 1 mm, we again get a y spread of about 0.05 microns, but this is a real blur. However, this is a small effect that probably can be neglected in almost all practical cases.

There is one more second-order aberration coefficient in lenses with bends that is zero in straight lenses: $T_{1,6,6} = \partial R_{1,6}/\partial\delta$. In the present double-triplet example with a bend angle of 0.2 degrees, $T_{1,6,6} = 0.13$ m. With an energy spread δ of 0.1%, this gives an image-plane x spread of 1.3×10^{-7} m, which when divided by the magnification is 1.3×10^{-8} m, a negligible blur term. This aberration coefficient has a linear dependence on bend angle.

6 Second approach: achromatic two-stage lens

With this approach, existing two-stage straight-lens quadrupole lengths and gradients, and drift lengths can be used essentially with no modification, except that the last part of the final drift of the first stage and the first part of the initial drift of the second stage are replaced by equal-length, equal strength half-dipoles. This centers the whole dipole at the image plane of the first stage, where both $R_{1,2} = 0$ and $R_{3,4} = 0$. Therefore Eq. 8 and its analog for bends in the y plane are both satisfied, and we can can have achromatic image steering in both the x and y planes, if desired. Since beamline data on compound lenses

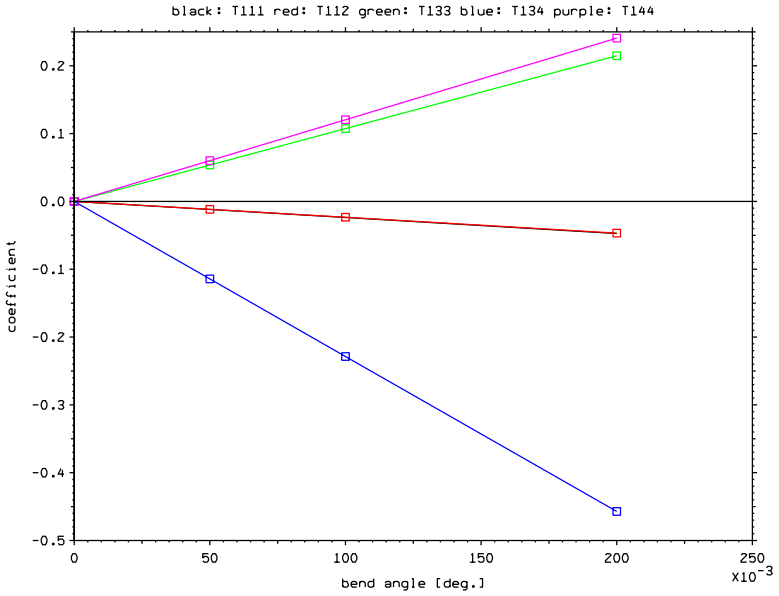

Figure 2: Dependence of second-order final-x geometric aberration coefficients on bend angle. Black curve: $T_{1,1,1}$; red curve: $T_{1,1,2}$; green curve: $T_{1,3,3}$; blue curve: $T_{1,3,4}$, and purple curve: $T_{1,4,4}$. The black and red curves almost overlap.

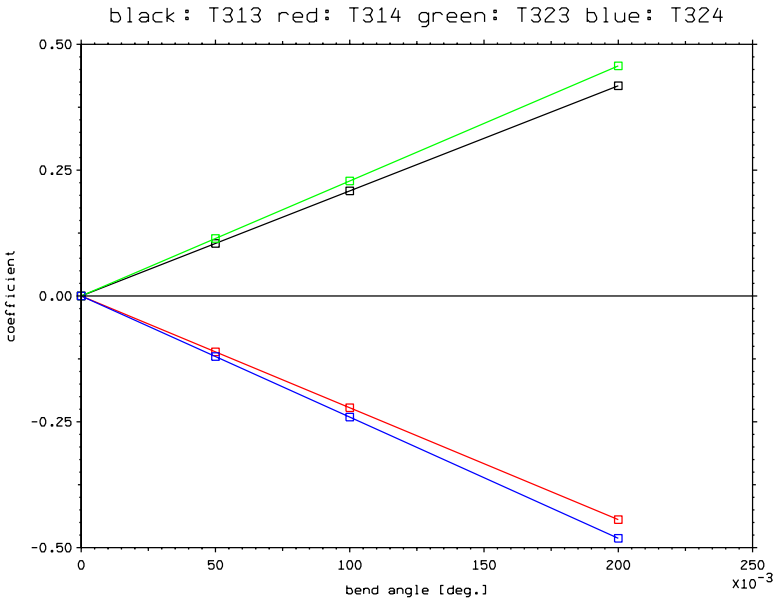

Figure 3: Dependence of second-order final-y geometric aberration coefficients on bend angle. Black curve: $T_{3,1,3}$; red curve: $T_{3,1,4}$; green curve: $T_{3,2,3}$, and blue curve: $T_{3,2,4}$.

```
            R matrix for compound lens with bend
 5.00000E+01 -5.32907E-15  0.00000E+00  0.00000E+00  0.00000E+00 -9.28077E-17
 2.64868E+00  2.00000E-02  0.00000E+00  0.00000E+00  0.00000E+00  3.49066E-04
 0.00000E+00  0.00000E+00  5.00000E+01  9.49796E-14  0.00000E+00  0.00000E+00
 0.00000E+00  0.00000E+00  2.65280E+00  2.00000E-02  0.00000E+00  0.00000E+00
-1.74533E-02  5.55521E-19  0.00000E+00  0.00000E+00  1.00000E+00  8.63989E-08
 0.00000E+00  0.00000E+00  0.00000E+00  0.00000E+00  0.00000E+00  1.00000E+00
```

have been previous reported [3], a beamline table will not be given here. The R matrix computed by Marylie for an achromatic compound magnifier with a first-stage magnification of -10 and a second-stage magnification of -5, with the bending dipole centered at the Stage 1 image plane, is given below. As in the doublet-triplet achromatic lens, the second-order geometric aberrations increase linearly with the bend angle, but the second-order chromatic aberrations (except for $T_{1,6,6}$) change very little with bend angle and are essentially the same as those in the equivalent no-bend lens. When they are divided by the magnification, they are only a little larger than those of the first stage of the lens, when it is used without a second stage (this is shown in Ref. [4]) . Since the second-stage length is about the same as the first-stage length and the magnification is larger, the required bend angle is larger than for the doublet-triplet lens for the same field-of-view in the object. However, when aberrations are divided by the magnification, the actual geometric aberration blur with the scaled-up bend angle about the same as that for the doublet-triplet lens, and should be negligible in most cases of interest. In summary, the compound (two-stage) achromatic weak-bend lens looks like a very promising approach for dealing with bremsstrahlung background.

7 References

[1] See David C. Carey, *The Optics of Charged-Particle Beams*, Harwood Academic Publishers, NY, 1987, Chapter 2. Note that Carey uses the momentum deviation $\delta = \delta p/p_0$, instead of the Marylie coordinate δ defined in Section 3. For particles traveling at nearly the speed of light, the main effect of this is to change the signs of R_{16} and R_{26}.

[2] C. T. Mottershead and J. D. Zumbro, "Magnetic Optics for Proton Radiography", proceedings of the 1997 Particle Accelerator Conference, May 12-17, Vancouver, BC, Canada, pp. 1397-1399.

[3] P. L. Walstrom, AOT-HPE Technical Note AOT-HPE:14-003, "High-Gradient Compound Quadrupole Lenses for 12 GeV Electron Radiography", Feb. 20, 2014

[4] P. L. Walstrom, AOT-HPE Technical Note AOT-HPE:14-004, "Second-Order Chromatic Coefficients for a Compound Lens", March 2014.